INTERNATIONAL JOURNAL FOR NUMERICAL METHODS IN FLUIDS
Int. J. Numer. Meth. Fluids 2009; **59**:195–213
Published online 28 April 2008 in Wiley InterScience (www.interscience.wiley.com). DOI: 10.1002/fld.1819

A coupled lattice Boltzmann model for the shallow water-contamination system

Yineng Li and Ping Huang*, †

Department of Environmental Science, School of Environmental Science and Engineering, Sun Yat-sen University, Guangzhou 510275, China

SUMMARY

A coupled numerical method for the direct simulation of shallow water dynamics and pollutant transport is formulated and implemented. The conservation equations of shallow water dynamics equations and the convection–diffusion equations are solved using the lattice Boltzmann (LB) method. The local equilibrium distribution of the pollutant has no terms of second order in flow velocity. And the relaxation time of the pollutant deviates from a constant for the flows with variable free surface water depth. The numerical tests show that this scheme strictly obeys the conservation law of mass and momentum. Excellent agreement is obtained between numerical predictions and analytical solutions in the pure diffusion problem and convection–diffusion problem. Furthermore, the influences on the accuracy of the lattice size and the diffusivity are also studied. The results indicate that the variation in the free surface water depth cannot affect the conservation of the model, and the model has the ability to simulate the complex topography problem. The comparison shows that the LB scheme has the capacity to solve the complex convection–diffusion problem in shallow water. Copyright © 2008 John Wiley & Sons, Ltd.

Received 10 April 2007; Revised 2 March 2008; Accepted 4 March 2008

KEY WORDS: coupled lattice Boltzmann method; shallow water equation; convection with diffusion; conservation law

1. INTRODUCTION

In the last two decades research on methods of solution to the shallow water equations has received considerable attention. The shallow water equations have wide applications in ocean and hydraulic engineering: tidal flows in estuary and coastal water regions; bore wave propagation; the stationary

*Correspondence to: Ping Huang, Department of Environmental Science, School of Environmental Science and Engineering, Sun Yat-sen University, Guangzhou 510275, China.
†E-mail: eeshping@mail.sysu.edu.cn, phph888@163.com

Contract/grant sponsor: Research Fund for the Doctoral Program of Higher Education; contract/grant number: 20060558060

Copyright © 2008 John Wiley & Sons, Ltd.

hydraulic jump; and river, reservoir, and open-channel flows. Recently, prediction of a pollutant transport in flows is a newness and an important subject in many industrial and environmental projects. Hence, simulation of pollutant transport in shallow water is receiving more and more attention.

In the last decade the lattice Boltzmann method (LBM) has been successfully applied to the analysis of a variety of complex physical phenomena, such as turbulent flow [1–3], natural convection [4], multi-component flows [5–7], and multi-phase flows [8]. Besides, some less complicated phenomena such as shallow water dynamics and convection–diffusion problem have also been studied [9–16]. Unlike conventional numerical methods based on discretization of macroscopic equations, LBM is based on microscopic model and mesoscopic kinetic equations [17, 18].

However, the coupled shallow water dynamics and convection–diffusion have hardly been studied. This is probably due to the vast reservoir of alternative finite element, finite difference, and finite volume schemes for solving the convection–diffusion problem. Hence, in this paper we investigate whether the LB methodology can be extended to the pollutant-shallow water system.

In earlier research, Shan [19] carried out numerical simulations of the Rayleigh–Benard convection by using the previously developed two-component LBM. He *et al.* [20] also developed a novel thermal LBM model based on a similar approach, in which an independent distribution function for internal energy is introduced to simulate the temperature field. In both models, however, the equilibrium distribution function for the temperature contains the terms of second order in flow velocity. Since the convection–diffusion equation has no terms of second order in flow velocity, it is sufficient to take account of the terms up to first order in flow velocity [21]. Inamuro *et al.* [22] present a simplified LBM to simulate fluid flows with heat and mass transfer and found that the model can be obtained with relative errors of the same order as the lattice spacing. However, in the practical water environment, the free surface water depth should be considered. Hence, in this paper a modified LBM is proposed for the convection–diffusion process with variation in free surface water depth in the shallow water.

A coupled lattice Boltzmann method (CLBM) for the pollutant-shallow water system is formulated and implemented using the modified local equilibrium distribution for pollutant convection and diffusion in this paper.

In the numerical computation, the CLBM scheme is firstly used to solve the 1-D and 2-D pure diffusion problems. Subsequently, the same framework is applied to the 1-D and 2-D convection–diffusion problem in 1-D and 2-D steady flow. The influences on the accuracy of the lattice size and the diffusivity are also studied.

2. GOVERNING EQUATIONS

The 2-D shallow water equations with source terms of bed slope and bed friction and the convection–diffusion equation may be expressed in tensor notation as

$$\frac{\partial \zeta}{\partial t} + \frac{\partial (hu_j)}{\partial x_j} = 0 \tag{1}$$

$$\frac{\partial (hu_i)}{\partial t} + \frac{\partial (hu_i u_j)}{\partial x_j} + \frac{\partial}{\partial x_i}\left(\frac{gh^2}{2}\right) = S_i + \nu\left[\frac{\partial}{\partial x_j}\frac{\partial}{\partial x_j}(hu_i) + \frac{\partial}{\partial x_i}\frac{\partial}{\partial x_j}(hu_j)\right] \tag{2}$$

Copyright © 2008 John Wiley & Sons, Ltd.

DOI: 10.1002/fld

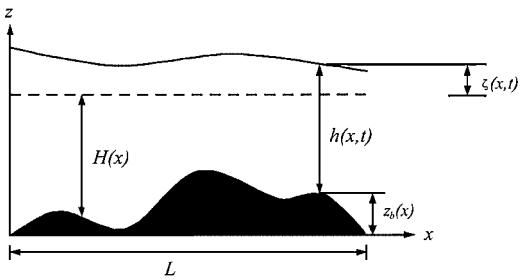

Figure 1. Definition sketch for bed topography.

$$\frac{\partial(hc)}{\partial t}+\frac{\partial(hu_j c)}{\partial x_j}=\frac{\partial}{\partial x_j}\left(Dh\frac{\partial c}{\partial x_j}\right)+S_c \tag{3}$$

where ζ is the free water surface elevation above a fixed reference water level; $h=H+\zeta$ is the total water depth with H being the partial depth between the fixed reference level and the bed surface (see Figure 1); i and j are indices and the Einstein summation convention is used, i.e. repeated indices mean a summation over the space coordinates; x_i is the Cartesian coordinate; u_i is depth-averaged velocity component in the i direction; g is the acceleration due to gravity; t is the time; c is the concentration-averaged; $g=9.81\,\mathrm{m/s^2}$ is the gravitational acceleration; v is the kinematic viscosity; and D is the coefficient of diffusion.

$$S_i=S_{bi}-S_{fi} \tag{4}$$

$$S_{bi}=-gh\frac{\partial z_b}{\partial x_i} \tag{5}$$

$$S_{fi}=gn^2u_i\sqrt{u_ju_j}/h^{1/3} \tag{6}$$

$$S_c=-Khc+S_0h \tag{7}$$

where z_b is the bed elevation above the datum; n is the Manning coefficient at the bed; K is the attenuation coefficient; and S_0 is the source term.

3. COUPLED LATTICE BOLTZMANN METHOD

3.1. LBM for the flow field

According to the theory of the LBM, it consists of two steps: a streaming step and a collision step [23]. The collision operator Ω is replaced with the single relaxation time τ under the Bhatnagar–Gross–Krook (BGK) approximation. Usually, with the BGK approximation [24] these two steps can be combined into the following lattice Boltzmann (LB) equation using the 9-speed square lattice shown in Figure 2:

$$f_\alpha(x_i+e_\alpha\Delta t,t+\Delta t)-f_\alpha(x_i,t)=-\frac{1}{\tau}(f_\alpha-f_\alpha^{\mathrm{eq}})+\frac{\Delta t}{N_\alpha e^2}e_\alpha F_\alpha(x_i,t)\quad(\alpha=0\text{–}8) \tag{8}$$

Copyright © 2008 John Wiley & Sons, Ltd.

DOI: 10.1002/fld

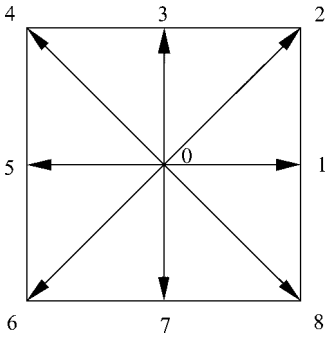

Figure 2. Discrete lattice and the trajectory of particles.

where f_α is the distribution function of particles; f_α^{eq} is the local equilibrium distribution function; $e=\Delta x/\Delta t$; Δx is the lattice size; Δt is the time step; F_α is the component of the force in the α direction; τ is the single relaxation time; e_α is the velocity vector of a particle in the α link; and N_α is a constant, which is decided by the lattice pattern as

$$N_\alpha=\frac{1}{e^2}\sum e_\alpha e_\alpha=6 \tag{9}$$

The physical variables, the water depth h and the velocity u, are defined in terms of the distribution function as

$$h=\sum_\alpha f_\alpha, \quad u=\frac{1}{h}\sum_\alpha e_\alpha f_\alpha \tag{10}$$

The velocity vector of particles is defined as

$$e_\alpha=\begin{cases} 0 & (\alpha=0) \\ \mathbf{i}e\cos\left(\dfrac{\pi(\alpha-1)}{4}\right)+\mathbf{j}e\sin\left(\dfrac{\pi(\alpha-1)}{4}\right) & (\alpha=1,3,5,7) \\ \mathbf{i}\sqrt{2}e\cos\left(\dfrac{\pi(\alpha-1)}{4}\right)+\mathbf{j}\sqrt{2}e\sin\left(\dfrac{\pi(\alpha-1)}{4}\right) & (\alpha=2,4,6,8) \end{cases} \tag{11}$$

The local equilibrium distribution f_α^{eq} for the shallow water equations is expressed as [9, 10]

$$f_\alpha^{\mathrm{eq}}=\begin{cases} h-\dfrac{5gh^2}{6e^2}-\dfrac{2h}{3e^2}u_iu_j & (\alpha=0) \\ \dfrac{gh^2}{6e^2}+\dfrac{h}{3e^2}e_{\alpha i}u_i+\dfrac{h}{2e^4}e_{\alpha i}e_{\alpha j}u_iu_j-\dfrac{h}{6e^2}u_iu_j\delta_{ij} & (\alpha=1,3,5,7) \\ \dfrac{gh^2}{24e^2}+\dfrac{h}{12e^2}e_{\alpha i}u_i+\dfrac{h}{8e^4}e_{\alpha i}e_{\alpha j}u_iu_j-\dfrac{h}{24e^2}u_iu_j\delta_{ij} & (\alpha=2,4,6,8) \end{cases} \tag{12}$$

where i and j are indices and the Einstein summation convention is used, i.e. repeated indices mean a summation over the space coordinates; the Kronecker delta δ_{ij} is $\delta_{ij}=1$ if $i=j$ and $\delta_{ij}=0$

Copyright © 2008 John Wiley & Sons, Ltd.

DOI: 10.1002/fld

if $i \neq j$. Hence, the local equilibrium function (12) satisfies the following conditions:

$$\sum_{\alpha} f_{\alpha}^{\mathrm{eq}} = h \tag{13}$$

$$\sum_{\alpha} e_{\alpha i} f_{\alpha}^{\mathrm{eq}} = h u_i \tag{14}$$

$$\sum_{\alpha} e_{\alpha i} e_{\alpha j} f_{\alpha}^{\mathrm{eq}} = \frac{1}{2} g h^2 \delta_{ij} + h u_i u_j \tag{15}$$

By applying the Chapman–Engkog procedure [25] and multi-scaling expansion, it can be shown that the solution to the LB equation (8) with the physical variables (10) and the equilibrium function (12) results in the solution to the shallow water equations (1) and (2) with

$$F_{\alpha}(x_i, t) = -gh \frac{\partial z_b}{\partial x_i} - S_{fi}, \quad v = \frac{\Delta t}{6}(2\tau - 1)e^2 \tag{16}$$

The time scale Δt should be chosen such that the ratio $U/e \ll 1$ is small enough to define a stable LB scheme. Here, U is the typical velocity of the flow.

3.2. LBM for the pollutant field

The local equilibrium distribution function for the convection–diffusion of contamination is defined as

$$g_{\alpha}^{\mathrm{eq}} = \begin{cases} c \cdot \left(h - \dfrac{5}{9} \right) & (\alpha = 0) \\ c \cdot \left(\dfrac{1}{9} + \dfrac{h}{3e^2} e_{\alpha i} u_i \right) & (\alpha = 1, 3, 5, 7) \\ c \cdot \left(\dfrac{1}{36} + \dfrac{h}{12e^2} e_{\alpha i} u_i \right) & (\alpha = 2, 4, 6, 8) \end{cases} \tag{17}$$

Therefore, the distribution function of particles for pollutant can be calculated using the following equation:

$$g_{\alpha}(x_i + e_{\alpha i} \Delta t, t + \Delta t) - g_{\alpha}(x_i, t) = -\frac{1}{\tau_c^*}(g_{\alpha} - g_{\alpha}^{\mathrm{eq}}) + \Delta t \cdot Sc_{\alpha}(x_i, t) \tag{18}$$

For the pollutant in shallow water with variable water depth, the relaxation time may deviate from a constant according to

$$\tau_c^* = \tfrac{1}{2} + h(x_i, t) \cdot (\tau_c - \tfrac{1}{2}) \tag{19}$$

$Sc_{\alpha}(x, t)$ is defined as

$$Sc_{\alpha}(x_i, t) = w_{\alpha} \cdot S_c \tag{20}$$

where $w_0 = \frac{4}{9}$, $w_{\alpha} = \frac{1}{9}$ for $\alpha = 1, 3, 5, 7$ and $w_{\alpha} = \frac{1}{36}$ for $\alpha = 2, 4, 6, 8$. With Equation (20) we have

$$\sum_{\alpha} Sc_{\alpha}(x_i, t) = S_c, \quad \sum_{\alpha} e_{\alpha i} \cdot Sc_{\alpha}(x_i, t) = 0 \tag{21}$$

Copyright © 2008 John Wiley & Sons, Ltd.

DOI: 10.1002/fld

The pollutant concentration c is defined as

$$c=\frac{1}{h}\sum_{\alpha} g_{\alpha} \tag{22}$$

By applying the multi-scaling expansion, it can be shown that the solution to the LB equation (18) with the equilibrium function (17) results in the solution to the convection–diffusion equation (3) with the coefficient of diffusion defined as (see Appendix A)

$$D=\frac{\Delta t}{6}(2\tau_c-1)e^2 \tag{23}$$

3.3. Boundary condition

The inflow and outflow boundary conditions for the flow field can be decided with the method described by Zou and He [26], using the given velocity, depth, and concentration to obtain the unknown distribution function at the boundary. For example, given the velocity at the inflow boundary, after streaming, the unknown f_1, f_2, and f_8 (see Figure 2) can be expressed as

$$f_1=f_5+\frac{2hu}{3e} \tag{24}$$

$$f_2=f_6+\frac{f_7-f_3}{2}+\frac{hu}{6e} \tag{25}$$

$$f_8=f_4+\frac{f_3-f_7}{2}+\frac{hu}{6e} \tag{26}$$

For the inflow and outflow boundary conditions for the pollutant field, we use the extrapolation method proposed by Guo *et al.* [27]. The basic idea of the extrapolation method is to decompose the distribution function g_α on the boundary node x_b into its equilibrium and non-equilibrium parts:

$$g_\alpha(x_b,t)=g_\alpha^{\mathrm{eq}}(x_b,t)+g_\alpha^{\mathrm{neq}}(x_b,t) \tag{27}$$

The non-equilibrium term g_α^{neq} represents the deviation from the equilibrium, which should be small ($|g_\alpha^{\mathrm{neq}}|\ll|g_\alpha^{\mathrm{eq}}|$). Hence, it is reasonable to assume that $g_\alpha^{\mathrm{neq}}=\Delta t g_\alpha^{(1)}$. Thus,

$$g_\alpha^{\mathrm{neq}}(x_b,t)=g_\alpha^{\mathrm{neq}}(x_f,t)+O(\Delta t^2)=g_\alpha(x_f,t)-g_\alpha^{\mathrm{eq}}(x_f,t)+O(\Delta t^2) \tag{28}$$

where x_f is the nearest neighbour fluid node of x_b.

If the concentration on the boundary node x_b is known, the unknown concentration distribution is given as

$$g_\alpha(x_b,t)=g_\alpha^{\mathrm{eq}}(x_b,t)+g_\alpha(x_f,t)-g_\alpha^{\mathrm{eq}}(x_f,t) \tag{29}$$

Alternately, if the concentration gradient is known on the boundary node x_b, $g_\alpha(x_b,t)$ is given as

$$g_\alpha(x_b,t)=\bar{g}_\alpha^{\mathrm{eq}}(x_b,t)+g_\alpha(x_f,t)-g_\alpha^{\mathrm{eq}}(x_f,t) \tag{30}$$

where $\bar{g}_\alpha^{\mathrm{eq}}(x_b,t)$ is an approximation to $g_\alpha^{\mathrm{eq}}(x_b,t)$ defined as

$$\bar{g}_\alpha^{\mathrm{eq}}(x_b,t)=[c(x_f,t)+(x_b-x_f)\cdot\nabla c(x_b,t)]\cdot w_\alpha\cdot\left[h+\frac{3he_\alpha u}{e^2}\right] \tag{31}$$

Copyright © 2008 John Wiley & Sons, Ltd.

DOI: 10.1002/fld

For the solid boundary condition, no-slip or slip boundary conditions are applied in the flow field and slip boundary condition is applied in the pollutant field. For the no-slip condition, the standard bounce-back scheme can be used. For the slip condition, a zero gradient of the distribution function normal to the solid wall can be used [28, 29].

4. NUMERICAL ANALYSIS

4.1. Pure diffusion tests

In this section the coupled LBM is used to solve the 1-D and 2-D pure diffusion problems. The accuracy is demonstrated by comparing numerical predictions with analytical solutions or finite difference solutions.

4.1.1. 1-D uniform concentration with variation in water depth. An 10 m long 0.5 m wide resting rectangle channel with water level $\zeta = 1$ m, velocity of flow $u = 0$ m/s, and the concentration $c = 1$ mg/L is presented for this example. The sketch of the channel is shown in Figure 3. As the initial concentration is uniform, the concentration will remain uniform as the time increases ($c \equiv 1$ mg/L). In the numerical computations, $e = 10$ m/s, $D = 0.01\,\text{m}^2/\text{s}$ ($\tau_c = 0.53$), $\Delta x = \Delta y = 0.1$ m, $\Delta t = 0.01$ s were used. Figure 4 shows the numerical solution to the concentration. After 1000 time steps, the

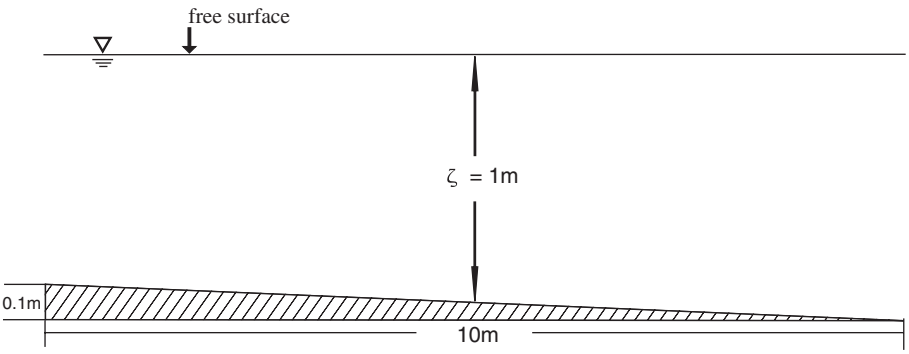

Figure 3. Sketch of the channel with variation in the bottom slope.

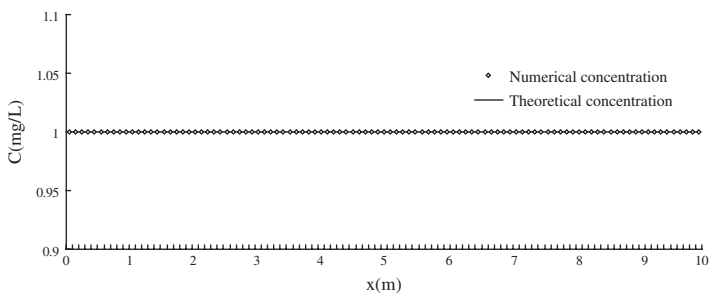

Figure 4. Initial uniform concentration: comparison of concentration.

Copyright © 2008 John Wiley & Sons, Ltd.

DOI: 10.1002/fld

concentration is still uniform with $c=1\,\mathrm{mg/L}$. This suggests that the variation in the free surface water depth cannot affect the conservation of the model.

4.1.2. 1-D pure diffusion test. A 1-D pure diffusion problem in an 8 m long 0.5 m wide resting rectangle channel with 1 g pollutant instantaneously (0.02 s) added into the middle of the channel is defined as [30]

$$c=\frac{m}{A}\cdot\frac{1}{\sqrt{2\pi}\sigma}\mathrm{e}^{-(x-x_0)^2/2\sigma^2} \tag{32}$$

where $m=10\,\mathrm{g}$ is the mass of the pollutant; $x_0=4\,\mathrm{m}$ is the location where the contamination is added into the channel; A is the area of the channel cross section, $\sigma^2=2Dt$ with D being defined using Equation (23).

The global relative error R is defined as

$$R=\frac{\sqrt{\sum_i |c_i-c_{ai}|^2}}{\sqrt{\sum_i |c_{ai}|^2}} \tag{33}$$

where c_i and c_{ai} are the numerical computation solution and the analytical solution, respectively.

The cases of the water depth $h=1$ and 2 were calculated. In the numerical computations, $e=5\,\mathrm{m/s}$, $x_0=4\,\mathrm{m}$, $\tau=0.51$. To test the effect of the lattice size on the solutions, three lattices $\Delta x=\Delta y=0.2\,\mathrm{m}$, $\Delta t=0.04\,\mathrm{s}$, $D=0.02\,\mathrm{m^2/s}$ ($\tau_c=0.56$); $\Delta x=\Delta y=0.1\,\mathrm{m}$, $\Delta t=0.02\,\mathrm{s}$, $D=0.02\,\mathrm{m^2/s}$ ($\tau_c=0.62$); and $\Delta x=\Delta y=0.05\,\mathrm{m}$, $\Delta t=0.01\,\mathrm{s}$, $D=0.02\,\mathrm{m^2/s}$ ($\tau_c=0.74$) were used in the initial computations. The 1-D diffusion can be guaranteed in the 2-D code by specifying slip boundary conditions at the sidewalls. The results of $t=2$ and 5 s are depicted in Figure 5, showing good agreement with the analytical solution. Further quantitative comparison with the analytical solution indicates that in the process of the diffusion the relative error becomes smaller with $R=2.19\mathrm{e}{-2}$ at $t=2\,\mathrm{s}$, $h=1\,\mathrm{m}$ and $R=1.51\mathrm{e}{-2}$ at $t=5\,\mathrm{s}$, $h=1\,\mathrm{m}$. Figure 6 shows the comparison between

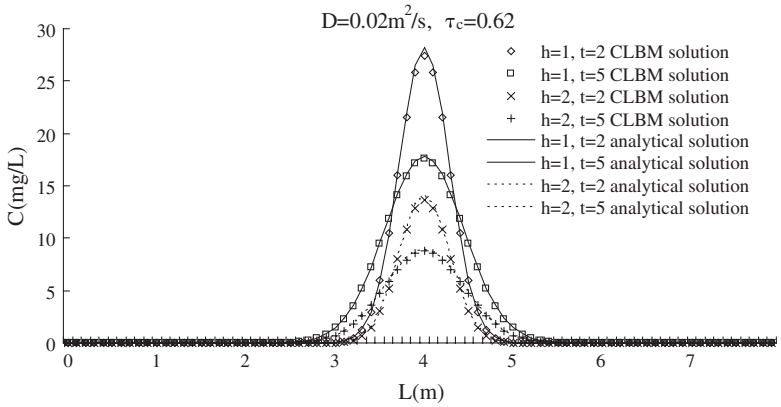

Figure 5. 1-D pure diffusion: comparison of concentration at 2 and 5 s ($h=1$ and 2 m).

Copyright © 2008 John Wiley & Sons, Ltd.

DOI: 10.1002/fld

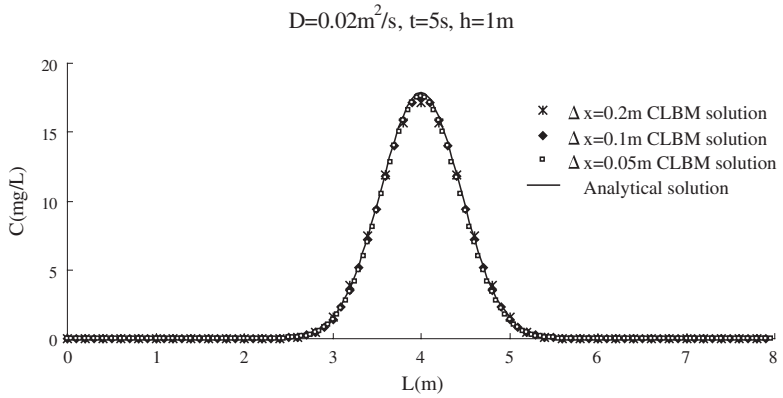

Figure 6. 1-D pure diffusion: comparison of concentration based on different lattices sizes.

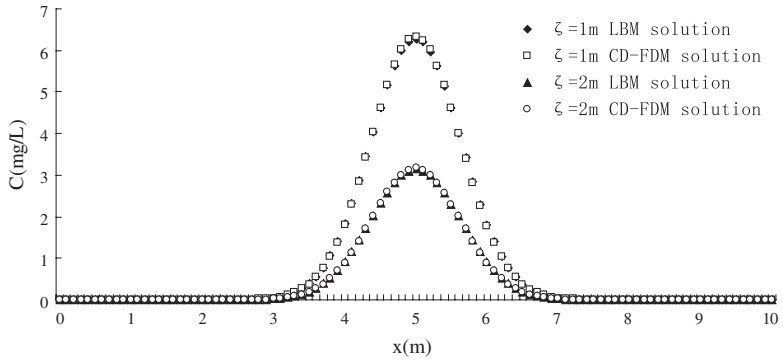

Figure 7. 1-D pure diffusion with varying bottom slope: comparison of concentration at 10 s ($\zeta = 1$ and 2 m).

numerical results based on different lattice sizes, showing that there is little difference. Further comparison indicates that the lattice $\Delta x = 0.05$ m has most accuracy with $R = 9.8\text{e}{-3}$ in $\Delta x = 0.05$ m, $R = 1.51\text{e}{-2}$ in $\Delta x = 0.1$ m, and $R = 3.14\text{e}{-2}$ in $\Delta x = 0.2$ m.

4.1.3. 1-D pure diffusion test with variation in water depth. This example changes the initial condition of the example in Section 4.1.1 to $c = 0$ mg/L. And 1 g pollutant was instantaneously (0.01 s) added into the middle of the channel. The velocity of flow is $u = 0$ m/s. The cases of the water level $\zeta = 1$ and 2 were calculated. In the numerical computations, $e = 10$ m/s, $D = 0.02\,\text{m}^2/\text{s}$ ($\tau_c = 0.56$), $\Delta x = \Delta y = 0.1$ m, and $\Delta t = 0.01$ s were used. The results after 1000 time steps ($t = 10$ s) compared with the solutions to central difference finite difference method (CD-FDM) are shown in Figure 7. They are in good agreement. This suggests that the model has the ability to simulate complex topography problem.

Copyright © 2008 John Wiley & Sons, Ltd.

DOI: 10.1002/fld

4.1.4. 2-D pure diffusion test. A 2-D pure diffusion problem in a $4\,\mathrm{m}\times 4\,\mathrm{m}$, 2 m deep quiet pool with pollutant added instantaneously (0.02 s) into the center of the pool is defined as [30]

$$c=\frac{m}{h}\cdot\frac{1}{2\pi\sigma^2}\mathrm{e}^{-[(x-x_0)^2+(y-y_0)^2]/2\sigma^2} \tag{34}$$

where $m=10\,\mathrm{g}$, $x_0=0$, $y_0=0$, and other parameters have the same meaning as Equation (32).

In the numerical computation, $\Delta x=\Delta y=0.1\,\mathrm{m}$, $\Delta t=0.02\,\mathrm{s}$, $e=5\,\mathrm{m/s}$, $x_0=2\,\mathrm{m}$, $\tau=0.52$, and $D=0.015\,\mathrm{m}^2/\mathrm{s}$ ($\tau_c=0.59$). The results of $t=10\,\mathrm{s}$ is depicted in Figure 8. The maximal absolute error is 0.0783 mg/L with the maximal numerical solution $C_{\max}$ being 5.30 mg/L, and the global relative error R is 9.3e−3. In addition, the smaller the lattice size used, the better the accuracy obtained ($R=2.0\mathrm{e}{-3}$ in the lattice $\Delta x=\Delta y=0.05\,\mathrm{m}$).

Further comparison of the lattice size and different diffusivity are presented in Table I. The smaller the lattice size and the larger the diffusivity used, the better the accuracy obtained. In Table I we can observe relatively good accuracy when $\mathrm{d}x/D<10$.

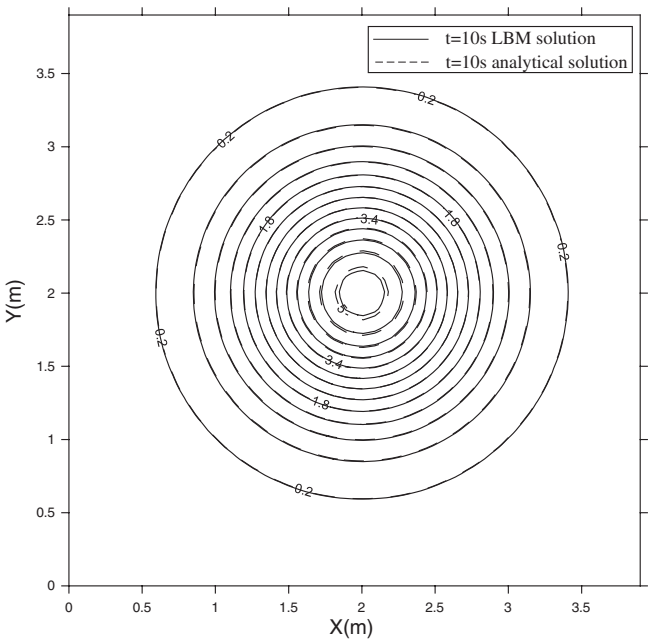

Figure 8. 2-D pure diffusion: comparison of concentration at 10 s.

Table I. 2-D pure diffusion: comparison of relative error for different lattice size and different diffusivity.

			Error R		
Δx (m)	e (m/s)	dt (s)	$D=0.005$	$D=0.01$	$D=0.02$
0.2	5.0	0.04	1.154e−1	5.88e−2	2.91e−2
0.1	5.0	0.02	2.99e−2	1.45e−2	8.0e−3
0.05	5.0	0.01	7.3e−3	3.3e−3	1.1e−3

Copyright © 2008 John Wiley & Sons, Ltd.

DOI: 10.1002/fld

4.2. Convection–diffusion tests

4.2.1. 1-D convective-diffusion problem with pollutant instantly discharging. In a $80\,\mathrm{m}\times 5\,\mathrm{m}$ flat channel with upriver discharge $Q=5.69\,\mathrm{m}^3/\mathrm{s}$ and downriver water depth $h=1.52\,\mathrm{m}$, 50 g non-degradable contamination is instantly discharged into the location $x_0=10\,\mathrm{m}$. This problem can be defined as [30]

$$c=\frac{m}{A}\cdot\frac{1}{\sqrt{2\pi}\sigma}\mathrm{e}^{-(x-x_0-ut)^2/2\sigma^2} \tag{35}$$

The parameters have the same meaning as Equation (32).

In the numerical computations, $\Delta x=\Delta y=1\,\mathrm{m}$, $\Delta t=0.1\,\mathrm{s}$, $e=10\,\mathrm{m/s}$, $\tau=0.53$, $D=0.4\,\mathrm{m}^2/\mathrm{s}$ ($\tau_c=0.62$), and $n=0.01$. Figure 9 shows the discharge comparison of the numerical solution and theoretical solution. The result shows excellent agreement with $R<1\mathrm{e}-5$. A comparison of the numerical results with the analytical solution at $t=20$, 40, and 60 s is shown in Figure 10, showing good agreement. With increasing time, the relative error becomes larger. $R=1.69\mathrm{e}-2$ at $t=20\,\mathrm{s}$, $R=1.89\mathrm{e}-2$ at $t=40\,\mathrm{s}$ and $R=2.51\mathrm{e}-2$ at $t=60\,\mathrm{s}$. This may be related to the maximum concentration becoming smaller as the time increases. Further calculation shows that the maximum absolute error is smaller than $0.0127\,\mathrm{mg/L}$ and the maximum computational concentration is $0.645\,\mathrm{mg/L}$. The present method can provide good accuracy in the convective-diffusion problem.

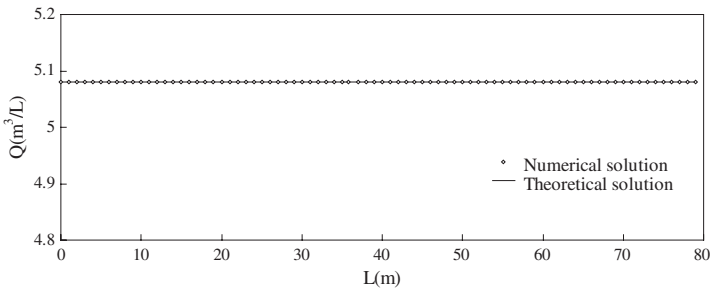

Figure 9. 1-D convective-diffusion: comparison of the discharge.

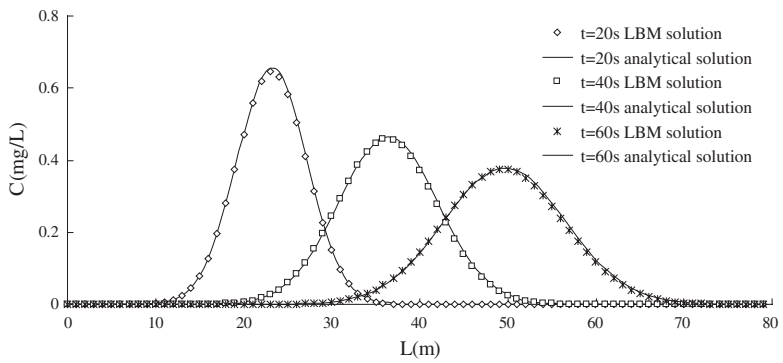

Figure 10. 1-D convective-diffusion: comparison of the concentration at 20, 40 and 60 s.

Copyright © 2008 John Wiley & Sons, Ltd.

DOI: 10.1002/fld

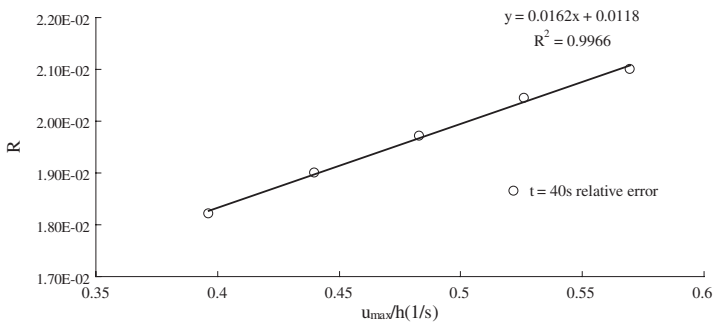

Figure 11. 1-D convective-diffusion: the relative error for different hydraulic boundary condition.

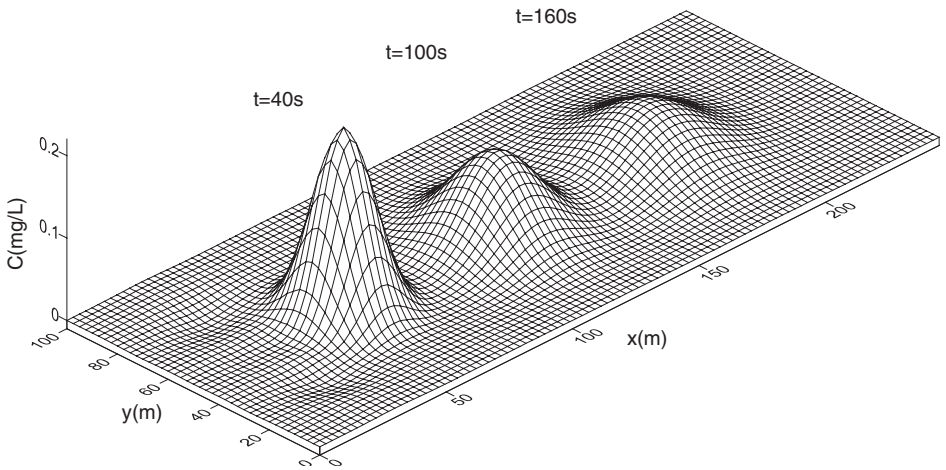

Figure 12. 2-D convection–diffusion: the concentration distribution at different times.

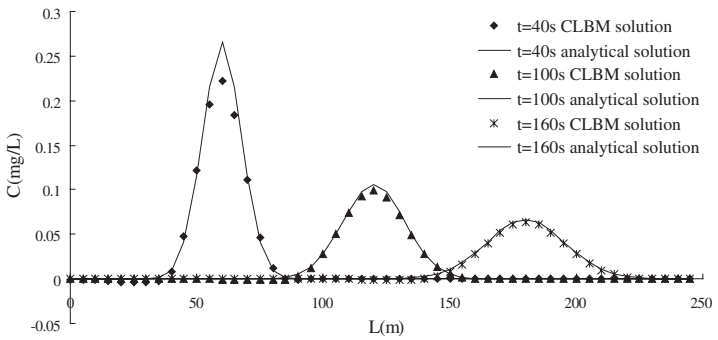

Figure 13. 2-D convection–diffusion: comparison of the concentration at different times.

Copyright © 2008 John Wiley & Sons, Ltd.

DOI: 10.1002/fld

Figure 11 shows the numerical relative error for different hydraulic boundary conditions. The results are linear. From the rule of the results we can see even when $u_{\max}/h = 1(1/\mathrm{s})$, the relative error will be less than 3e−2. Hence, the results show high accuracy of the model.

4.2.2. 2-D convection–diffusion in 1-D flow. (1) *Instant source*: Hundred gram of pollutant was instantly added into the channel. The water depth is 1 m; the velocity is 1 m/s. $\Delta x = \Delta y = 5\,\mathrm{m}$, $e = 10\,\mathrm{m/s}$, $\tau = 0.52$, and $D = 0.75\,\mathrm{m}^2/\mathrm{s}$ ($\tau_c = 0.545$). The results of $t = 40, 100$, and 160 s are shown in Figure 12. Comparison with the analytical solution is presented in Figure 13. We can see the results accord with the convection–diffusion law. The results show that the model has good accuracy for the 2-D convection–diffusion.

(2) *Continuum source*: In this example, a pollutant discharge outlet is in the side of the channel with a discharge amount of 100 g/s. The discharge per unit width of $q = 1\,\mathrm{m}^2/\mathrm{s}$ was imposed at the inflow and $h = 1.52\,\mathrm{m}$ was specified at the downstream end. $e = 10\,\mathrm{m/s}$, $\tau = 0.53$, $n = 0.01$,

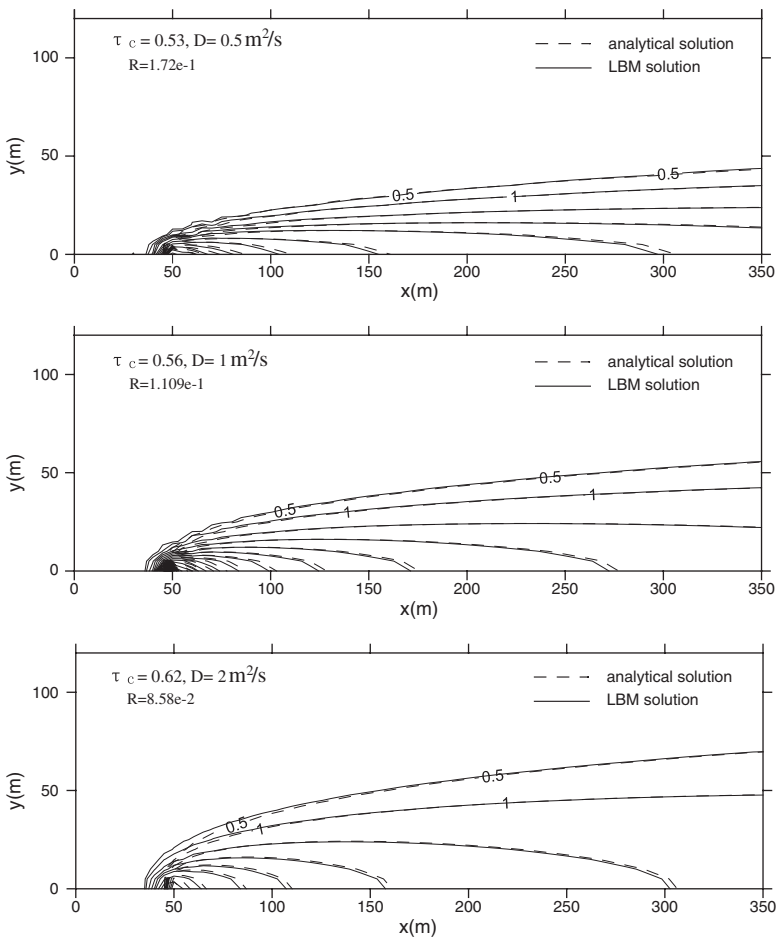

Figure 14. 2-D convection–diffusion: comparison of the concentration for different relaxation times.

Copyright © 2008 John Wiley & Sons, Ltd.

DOI: 10.1002/fld

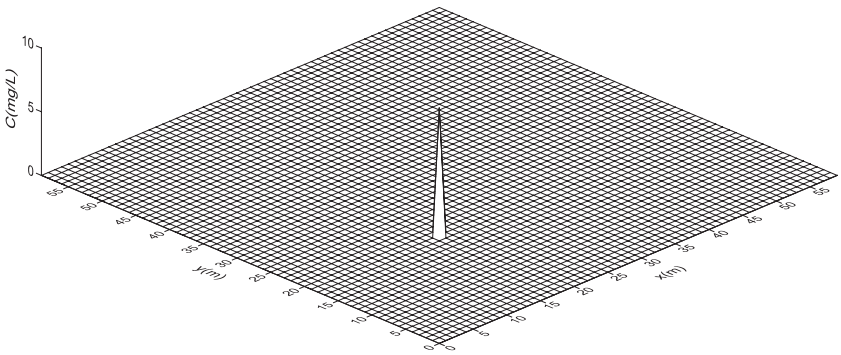

Figure 15. Initial concentration surface with $u = 1\,\mathrm{m/s}$ and $v = 1\,\mathrm{m/s}$.

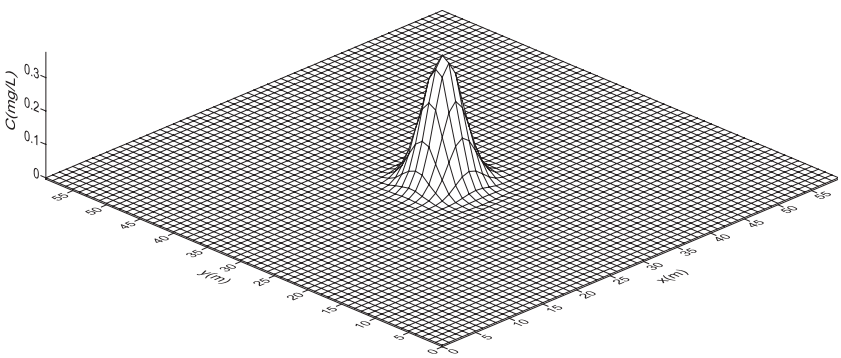

Figure 16. Predicted concentration surface at $t = 10\,\mathrm{s}$.

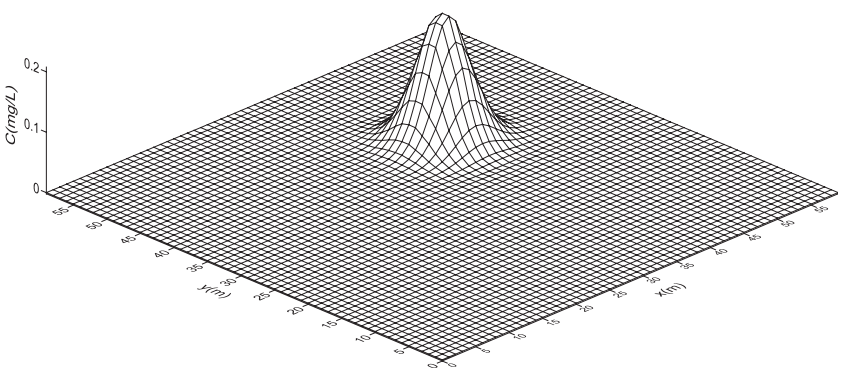

Figure 17. Predicted concentration surface at $t = 20\,\mathrm{s}$.

Copyright © 2008 John Wiley & Sons, Ltd.

DOI: 10.1002/fld

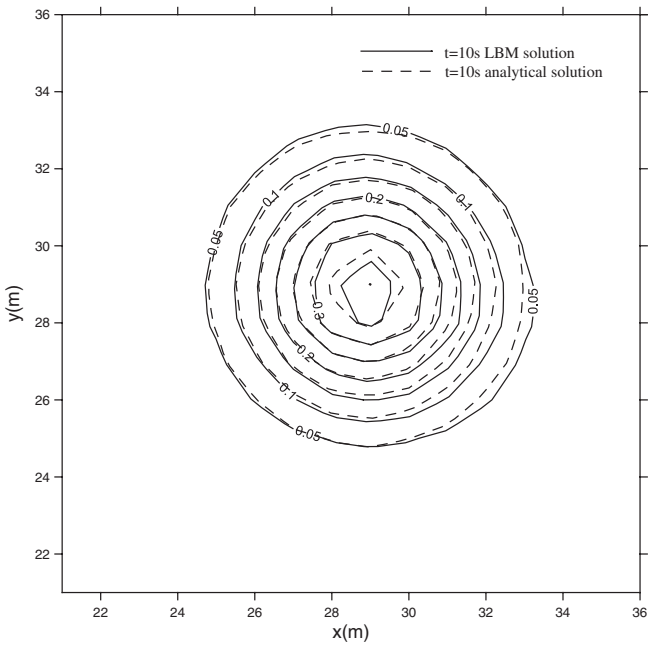

Figure 18. Comparison of concentration with $u = 1\,\mathrm{m/s}$ and $v = 1\,\mathrm{m/s}$ at 10 s.

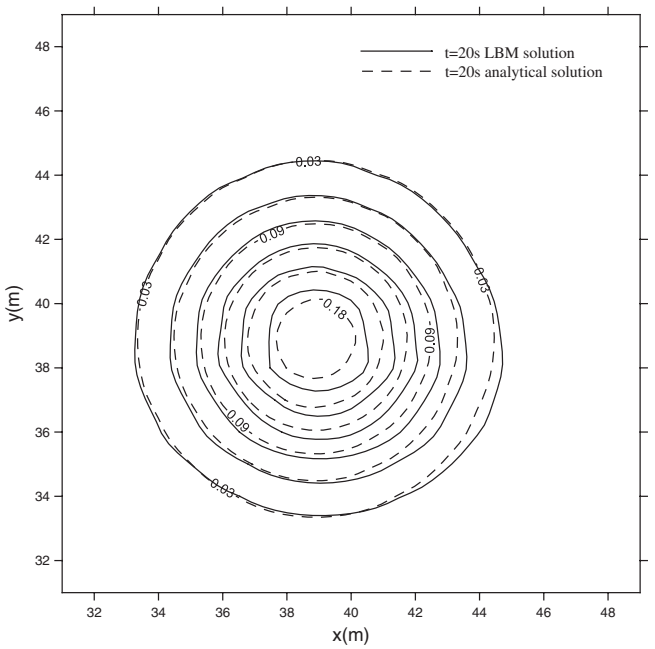

Figure 19. Comparison of concentration with $u = 1\,\mathrm{m/s}$ and $v = 1\,\mathrm{m/s}$ at 20 s.

Copyright © 2008 John Wiley & Sons, Ltd.

DOI: 10.1002/fld

$K=0.1/86400\,1/\mathrm{s}$, and $\Delta x=\Delta y=5\,\mathrm{m}$. To test the effect of the diffusivity on the solutions, $D=0.5\,\mathrm{m}^2/\mathrm{s}$ ($\tau_c=0.53$), $D=1\,\mathrm{m}^2/\mathrm{s}$ ($\tau_c=0.56$), and $D=2\,\mathrm{m}^2/\mathrm{s}$ ($\tau_c=0.62$) were used in the initial computations. Comparisons between numerical results and analytical solution are depicted in Figure 14, showing that there is little difference and the major difference is near the pollutant discharge outlet. Further comparison indicates that the larger the diffusivity, the less the difference from the analytical solution. The results suggest that the model is accurate in this problem.

4.2.3. 2-D convection–diffusion in 2-D flow. Simulating pollutant transport and diffusion in a $60\Delta x\times 60\Delta y$ square with the water depth of 1 m, the velocity $u=1\,\mathrm{m/s}$ and $v=1\,\mathrm{m/s}$. $\Delta x=\Delta y=1\,\mathrm{m}$, $e=10\,\mathrm{m/s}$, $\tau=0.52$, $D=0.2\,\mathrm{m}^2/\mathrm{s}$ ($\tau_c=0.56$). Ten gram of pollutant was instantly added into the test domain located at $x=20\,\mathrm{m}$ and $y=20\,\mathrm{m}$. The initial concentration distribution surface is shown in Figure 15. The results of $t=10$ and 20 s are shown in Figures 16 and 17, respectively. Figures 18 and 19 compare the computed concentration profiles with analytical solutions. The results show that the model has good accuracy for the 2-D convection–diffusion in 2-D flow.

5. CONCLUSION

A coupled LB model for the flow-pollutant system has been presented. The local equilibrium distributions proposed for the pollutant field are presented in a simplified form with no terms of second order in flow velocity. The relaxation time of the pollutant deviates from a constant for the flows with variable free surface water depth.

Numerical simulations of the 1-D and 2-D pure diffusion problems were carried out to test the model. The numerical results agree well with the analytical solution. The numerical results for the 1-D and 2-D convection–diffusion problems show good agreement with the analytical and high accuracy of the model. Influences on the accuracy of the lattice size and the diffusivity are also studied.

The uniform results of concentration in a varying water depth channel with uniform initial concentration indicate that the varying of the free surface water depth cannot affect the conservation of the model, and comparison with finite difference method indicates that the model has the ability to simulate complex topography problem.

The present CLBM can be used to solve the more complex practical problem and easily extended to the 3-D model. Such an extension and applications will be considered in future studies.

APPENDIX A: CALCULATING THE COEFFICIENT OF DIFFUSION

The local equilibrium distribution function for the convection–diffusion of contamination is defined as

$$g_\alpha^{\mathrm{eq}}=\begin{cases} c\cdot\left(h-\dfrac{5}{9}\right) & (\alpha=0)\\ c\cdot\left(\dfrac{1}{9}+\dfrac{h}{3e^2}e_{\alpha i}u_i\right) & (\alpha=1,3,5,7)\\ c\cdot\left(\dfrac{1}{36}+\dfrac{h}{12e^2}e_{\alpha i}u_i\right) & (\alpha=2,4,6,8)\end{cases} \tag{A1}$$

Copyright © 2008 John Wiley & Sons, Ltd.

DOI: 10.1002/fld

Therefore, the distribution function of particles for contamination can be calculated using the following equation:

$$g_\alpha(x_i+e_{\alpha i}\Delta t, t+\Delta t)-g_\alpha(x_i,t)=-\frac{1}{\tau_c^*}(g_\alpha-g_\alpha^{\mathrm{eq}})+\Delta t\cdot Sc_\alpha(x_i,t) \tag{A2}$$

The pollutant concentration c is defined as

$$c=\frac{1}{h}\sum_\alpha g_\alpha=\frac{1}{h}\sum_\alpha g_\alpha^{\mathrm{eq}} \tag{A3}$$

We unfurl Equation (A2) by the Taylor expansion

$$\Delta t\left[\frac{\partial}{\partial t}+(e_\alpha\cdot\nabla)\right]g_\alpha+\frac{\Delta t^2}{2}\left[\frac{\partial}{\partial t}+(e_\alpha\cdot\nabla)\right]^2 g_\alpha+O(\Delta t^3)=-\frac{1}{\tau_c^*}[g_\alpha-g_\alpha^{\mathrm{eq}}]+\Delta t\cdot Sc_\alpha \tag{A4}$$

By applying the Chapman–Engkog procedure and multiple scales expansion [25]

$$g_\alpha=g_\alpha^{\mathrm{eq}}+\varepsilon\cdot g_\alpha^{(1)}+\varepsilon^2 g_\alpha^{(2)}+\cdots \tag{A5}$$

$$\frac{\partial}{\partial t}=\frac{\partial}{\partial t_1}+\varepsilon\frac{\partial}{\partial t_2} \tag{A6}$$

where ε is the Knudsen number, a small number in the same order as Δt. We assume that $\varepsilon=\Delta t$. The above expansion assumes that the time scale t_2 is much slower than the time scale t_1 [17]. Substituting Equations (A5) and (A6) to Equation (A4), we have the ε order equation

$$\left[\frac{\partial}{\partial t_1}+(e_\alpha\cdot\nabla)\right]g_\alpha^{\mathrm{eq}}=-\frac{1}{\tau_c^*}g_\alpha^{(1)}+Sc_\alpha \tag{A7}$$

By using Equation (A7), we can have the ε^2 step equation

$$\frac{\partial}{\partial t_2}g_\alpha^{\mathrm{eq}}+\left[\frac{\partial}{\partial t_1}+(e_\alpha\cdot\nabla)\right]g_\alpha^{(1)}+\frac{1}{2}\left[\frac{\partial}{\partial t_1}+(e_\alpha\cdot\nabla)\right]^2 g_\alpha^{\mathrm{eq}}=-\frac{g_\alpha^{(2)}}{\tau_c^*} \tag{A8}$$

Considering Equation (A3) and $\sum 1/\tau_c^*(g_\alpha-g_\alpha^{\mathrm{eq}})=0$, we have the following equations:

$$\sum_\alpha\frac{1}{\tau_c^*}g_\alpha^{(n)}=0,\quad \sum_\alpha\frac{1}{\tau_c^*}e_\alpha\cdot g_\alpha^{(n)}=0\ \ (n=1,2\ldots) \tag{A9}$$

Considering Equations (12) and (A1), we can obtain

$$\sum_\alpha e_\alpha^2 g_\alpha^{\mathrm{eq}}=\frac{1}{3}e^2 c \tag{A10}$$

Calculating (A7) + $\varepsilon\times$ (A8)

$$\left[\varepsilon\frac{\partial}{\partial t_2}+\frac{\partial}{\partial t_1}+(e_\alpha\cdot\nabla)\right]g_\alpha^{\mathrm{eq}}-\varepsilon\left[\frac{\partial}{\partial t_1}+(e_\alpha\cdot\nabla)\right]\left[\tau_c^*\left(\frac{\partial}{\partial t_1}+e_\alpha\cdot\nabla\right)\right]g_\alpha^{\mathrm{eq}}$$
$$+\frac{\varepsilon}{2}\left[\frac{\partial}{\partial t_1}+(e_\alpha\cdot\nabla)\right]^2 g_\alpha^{\mathrm{eq}}+\left[\frac{\partial}{\partial t_1}+(e_\alpha\cdot\nabla)\right](\varepsilon\tau_c^* Sc_\alpha)=-\frac{g_\alpha^{(1)}+\varepsilon g_\alpha^{(2)}}{\tau_c^*}+Sc_\alpha \tag{A11}$$

Copyright © 2008 John Wiley & Sons, Ltd.

DOI: 10.1002/fld

Applying Equation (19) to Equation (A11)

$$\left[\varepsilon\frac{\partial}{\partial t_2}+\frac{\partial}{\partial t_1}+(e_\alpha\cdot\nabla)\right]g_\alpha^{\mathrm{eq}}-\left[\frac{\partial}{\partial t_1}+(e_\alpha\cdot\nabla)\right]\left[\varepsilon h\left(\tau_c-\frac{1}{2}\right)\left(\frac{\partial}{\partial t_1}+e_\alpha\cdot\nabla\right)\right]g_\alpha^{\mathrm{eq}}$$
$$+\left[\frac{\partial}{\partial t_1}+(e_\alpha\cdot\nabla)\right](\varepsilon\tau_c^* Sc_\alpha)=-\frac{g_\alpha^{(1)}+\varepsilon g_\alpha^{(2)}}{\tau_c^*}+Sc_\alpha \tag{A12}$$

Then we sum up Equation (A12) with Equations (A3), (A9), (21), and (A10)

$$\frac{\partial(hc)}{\partial t}+\frac{\partial(hu_j c)}{\partial x_j}=\frac{\partial}{\partial t_1}\sum_\alpha\left[\varepsilon h\left(\tau_c-\frac{1}{2}\right)\left(\frac{\partial}{\partial t_1}+e_\alpha\cdot\nabla\right)g_\alpha^{\mathrm{eq}}\right]+\nabla\cdot\sum_\alpha\left[\varepsilon h\left(\tau_c-\frac{1}{2}\right)e_\alpha\frac{\partial g_\alpha^{\mathrm{eq}}}{\partial t_1}\right]$$
$$-\frac{\partial}{\partial t_1}\sum_\alpha(\varepsilon\tau_c^* Sc_\alpha)+\nabla\left[\frac{\varepsilon he^2}{3}\left(\tau_c-\frac{1}{2}\right)\nabla(c)\right]+S_c \tag{A13}$$

The first three terms on the right-hand side of Equation (A13) are small compared with the fourth term as ∂t_1 is smaller than ∂t_2 and ∂x_i [13]. Therefore, they are treated as truncation errors. The closer τ_c is to $\frac{1}{2}$, the smaller the truncation. Then we have

$$\frac{\partial(hc)}{\partial t}+\frac{\partial(hu_j c)}{\partial x_j}=\frac{\partial}{\partial x_j}\left[\frac{\varepsilon he^2}{3}\left(\tau_c-\frac{1}{2}\right)\frac{\partial c}{\partial x_j}\right]+S_c \tag{A14}$$

Then it results in the solution to convection–diffusion equation (3):

$$\frac{\partial(hc)}{\partial t}+\frac{\partial(hu_j c)}{\partial x_j}=\frac{\partial}{\partial x_j}\left(Dh\frac{\partial c}{\partial x_j}\right)+S_c \tag{A15}$$

where the coefficient of diffusion

$$D=\frac{\Delta t}{6}(2\tau_c-1)\cdot e^2 \tag{A16}$$

ACKNOWLEDGEMENTS

The Research Fund for the Doctoral Program of Higher Education (RFDP) under project number 20060558060 is gratefully acknowledged.

REFERENCES

1. Filippova O, Succi S, Mazzocco F, Arrighetti C, Bella G, Hänel D. Multiscale lattice Boltzmann schemes with turbulence modeling. *Journal of Computational Physics* 2001; **170**:812–829.
2. Yu H, Girimaji S, Luo L. DNS and LES of decaying isotropic turbulence with and without frame rotation using lattice Boltzmann method. *Journal of Computational Physics* 2005; **209**:599–616.
3. Zhou JG. A lattice Boltzmann model for the shallow water equations with turbulence modeling. *International Journal of Modern Physics C* 2002; **13**:1135–1150.
4. Eggles GJM, Somers JA. Numerical simulation of free convective flow using the lattice-Boltzmann scheme. *International Journal of Heat and Fluid Flow* 1995; **16**:357–364.
5. Rothman DH, Keller JM. Immiscible cellular-automaton fluids. *Journal of Statistical Physics* 1988; **52**:1119–1127.
6. Holme R, Rothman DH. Lattice-gas and lattice-Boltzmann models of miscible fluids. *Journal of Statistical Physics* 1992; **68**:409–429.

Copyright © 2008 John Wiley & Sons, Ltd.

DOI: 10.1002/fld

7. Shan X, Doolen G. Multicomponent lattice-Boltzmann model with interparticle interaction. *Journal of Statistical Physics* 1995; **81**:379–397.
8. Hou S, Shan X, Zou Q, Doolen GD, Soll WE. Evaluation of two lattice Boltzmann models for multiphase flows. *Journal of Computational Physics* 1997; **138**:695–713.
9. Salmon R. The lattice Boltzmann method as a basis for ocean circulation modeling. *Journal of Marine Research* 1999; **57**:503–535.
10. Dellar PJ. Nonhydrodynamic modes and a priori construction of shallow water lattice Boltzmann equations. *Physical Review E* 2002; **65**:03609.
11. Zhou JG. A lattice Boltzmann model for the shallow water equations. *Computer Methods in Applied Mechanics and Engineering* 2002; **191**:3527–3539.
12. Chen YG, Suo LS. A lattice BGK model for simulating one-dimensional unsteady open channel flows. *Advances in Water Science* 2000; **11**(4):362–367.
13. Chen S, Dawson SP, Doolen GD, Janecky DR, Lawniczak A. Lattice methods and their applications to reacting systems. *Computers and Chemical Engineering* 1995; **19**:617–646.
14. Benjamin KC, David RN. A direct simulation method for particle-fluid systems. *Engineering Computations* 2004; **21**:151–168.
15. Wolf-Gladrow D. A lattice Boltzmann equation for diffusion. *Journal of Statistical Physics* 1995; **79**(5/6): 1023–1032.
16. Van der Sman RGM. Solving the vent hole design problem with a convection–diffusion lattice Boltzmann scheme. *International Journal of Computational Fluid Dynamics* 1999; **11**(3–4):237–248.
17. Chen S, Doolen GD. Lattice Boltzmann method for fluid flows. *Annual Review of Fluid Mechanics* 1998; **30**:329–364.
18. He X, Luo L. Lattice Boltzmann model for the incompressible Navier–Stokes equation. *Journal of Statistical Physics* 1997; **88**:927–944.13.
19. Shan X. Simulation of Rayleigh–Benard convection using a lattice Boltzmann method. *Physical Review E* 1997; **55**:2780–2788.
20. He X, Chen S, Doolen GD. A novel thermal model for the lattice Boltzmann method in incompressible limit. *Journal of Computational Physics* 1998; **146**:282–300.
21. Rothman DH, Zaleski S. *Lattice-gas Cellular Automata*. Cambridge University Press: Cambridge, U.K., 1997.
22. Inamuro T, Yoshino M, Inoue H, Mizuno R, Ogino F. A lattice Boltzmann method for a binary miscible fluid mixture and its application to a heat-transfer problem. *Journal of Computational Physics* 2002; **179**:201–215.
23. Benzi R, Succi S, Vergassola M. The lattice Boltzmann equation: theory and applications. *Physics Reports* 1992; **222**:45–197.
24. Bhatnager PL, Gross EP, Krook M. A model for collision processes in gases I. Small amplitude processes in charged and neutral one component system. *Physical Review* 1954; **94**:511–524.
25. Chapman S, Cowing TG. *The Mathematical Theory of Non-uniform Gases*. Cambridge University Press: Cambridge, U.K., 1939; 448.
26. Zou Q, He X. On pressure and velocity boundary conditions for the lattice Boltzmann BGK model. *Physics of Fluids* 1997; **9**:1591–1598.
27. Guo ZL, Shi BC, Zheng CG. A coupled lattice BGK model for the Boussinesq equations. *International Journal for Numerical Methods in Fluids* 2002; **39**:325–342.
28. Gallivan MA, Noble DR, Georgiads JG, Buckius RO. An evaluation of the bounce-back boundary condition for lattice Boltzmann simulations. *International Journal for Numerical Methods in Fluids* 1997; **25**:249–263.
29. He X, Zou Q, Luo L, Dembo M. Analytic solutions of simple flows and analysis of non slip boundary conditions for the lattice Boltzmann BGK Model. *Journal of Statistical Physics* 1997; **87**:115–136.
30. Huang P. *Water Environmental Mathematic Model and its Application*. Guangzhou Press: Guangzhou, China, 1996; 117–119.

Copyright © 2008 John Wiley & Sons, Ltd.

DOI: 10.1002/fld